MODELING O AND N ALLOYING IN Nb FOR SRF APPLICATIONS*

E.M. Lechner[†,1], J.W. Angle[2], A.D. Palczewski[1], F. A. Stevie[3], M. J. Kelley[1,2], and C. E. Reece[1]

[1] Thomas Jefferson National Accelerator Facility, Newport News, VA, USA
[2] Virginia Polytechnic Institute and State University, Blacksburg, VA, USA
[3] Analytical Instrumentation Facility, North Carolina State University, Raleigh, NC, USA

Abstract

Impurity alloying Nb has ushered in highly efficient superconducting radio frequency cavities. Modeling impurity diffusion profiles for superconducting radio frequency (SRF) applications will be crucial for developing next generation accelerators and engaging with modern theories to enhance performance. Here we describe modeling of oxygen and nitrogen alloying in Nb.

INTRODUCTION

Superconducting radio frequency cavities are the building blocks of contemporary particle accelerators. Major particle accelerators utilize SRF technology to facilitate fundamental research. In Nb SRF cavities, trace impurities can have tremendous impact. With quality factors, Qo, exceeding the previous state of the art by 2-4, LCLS-II and LCLS-II HE [1, 2] will employ nitrogen-alloyed Nb for their continuous wave accelerators. A goal remains to develop impurity diffusion models to tune interstitials optimally to modify Q_0 and E_{acc} for an intended application. This work requires the use of secondary ion mass spectrometry (SIMS). The high depth resolution and ability to quantify trace impurities makes SIMS the premier tool for testing diffusion models and parameter determination using the measured impurity depth profiles.

While Nb approaches its intrinsic limits, an opportunity presents itself to explore its ultimate limits via impurity management and nanostructuring [3-9] to reduce the surface resistance and increase the accelerating gradient. An important vector of RF surface resistance modification is electron mean free path tuning via alloying using various impurities [10-16]. Impurities greatly affect sensitivity to trapped flux [17-20] and a normal-conducting hydride precipitate blocking effect [21-24] which constitutes another vector of RF surface resistance optimization which must be carefully considered in managing impurities. Thorough exploration of these topics will optimize SRF properties for Nb and the lessons learned may be applicable to future materials [25, 26] in an effort to reduce the footprint and capital cost of future accelerators.

EXPERIMENTAL

SIMS measurements were made using a CAMECA 7f Geo magnetic sector SIMS instrument on Nb samples as described elsewhere [27]. The primary ion beam, made of Cs^+, is accelerated using a potential of 5 kV and sample potential of -3 kV for an impact energy of 8 keV. The Cs^+ ion beam was rastered over an area of 150×150 μm² with the collected data coming from a 63×63 μm² area in the center of the larger raster. Quantitation of the SIMS oxygen depth profiles was made using an implant standard to convert the ion signal to impurity concentration [28, 29]. Here, we used an O implant standard dosed with O at 2×10^{15} atoms/cm² at 180 keV by Leonard Kroko Inc to quantify the O composition of the RF penetration layer and beyond by detecting $^{16}O^-$ in conjunction with a $^{93}Nb^-$ reference signal.

NITROGEN ALLOYING

Alloying a Nb SRF cavity with N involves vacuum heat treating the cavity at 800 °C for 3 hours for H degas, exposure to N at 800 °C and a post-alloy anneal as shown in Fig. 1. After heat treatment, the cavity is electropolished 5-7 μm to remove lossy phases on the surface. Gonnella *et al*. [30, 31] showed that a diffusion model [32] fit their SIMS data reasonably well at depths greater than 10 μm, but was incapable of reproducing a depletion of interstitial N near the surface. No further modeling was pursued.
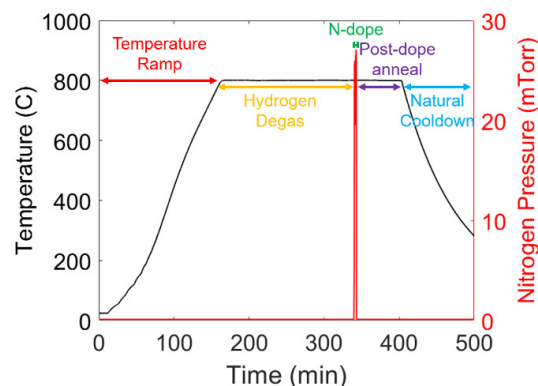

Figure 1: Furnace temperature and pressure profile relevant for N-alloying of Nb SRF cavities.

The N diffusion model of [32] accounts for a two-phase system consisting of a growing nitride layer on the surface and interstitial N migrating toward the bulk. Given nitrides populate the surface in such doping schemes for SRF [13], such a diffusion model may be a good starting point, however several convenient approximations are voluntarily forfeited when the alloying is chosen to be performed during a short time compared to the annealing process and furnace cooldown. These facts require that a model of N alloying relevant for SRF cavities must incorporate the following: 1. A sink term describing the depletion of N near the surface. 2. An annealing step. 3. Accurate understanding of N uptake. 4. Accurate understanding of the N diffusion coefficient.

A method of solution to describe this system can start with the model of [32] in the metal. The concentration of N is given by

$$c_m = C'_m - \frac{C''_m - C'_m}{erfc(\gamma_n\sqrt{\phi})} erfc\left(\frac{x}{2\sqrt{D_m t_D}}\right) \quad (1)$$

where c_m, C'_m, C''_m, C''_n, C''_n, and $C_n(\infty)$ are nitrogen concentration boundary conditions, γ_n and ϕ are proportionality constants, t_D is the doping time, D_n and D_m are the diffusion coefficients [32]. Equation 1 sets up the initial concentration profile, shown in Fig. 2(a) in blue, and used to advance to completion of an annealing step under a new diffusion equation with a sink

$$\frac{\partial c}{\partial t_A} = D_m \frac{\partial^2 c}{\partial x^2} + S. \quad (2)$$

The solution of this annealing step is shown in Fig. 2(a) in red and the evolution of the diffusion equation from our initial condition in blue to red is shown in Fig. 2(b). Here S is the sink term describing the removal of nitrogen at the surface which could be due to a reduction of solubility at reduced N pressure and temperature [33] or condensation of nitrides, and t_A is the annealing time. Using this solution scheme, it is possible to incorporate the aforementioned requirements for an adequate diffusion model for this system as shown in Fig. 2.
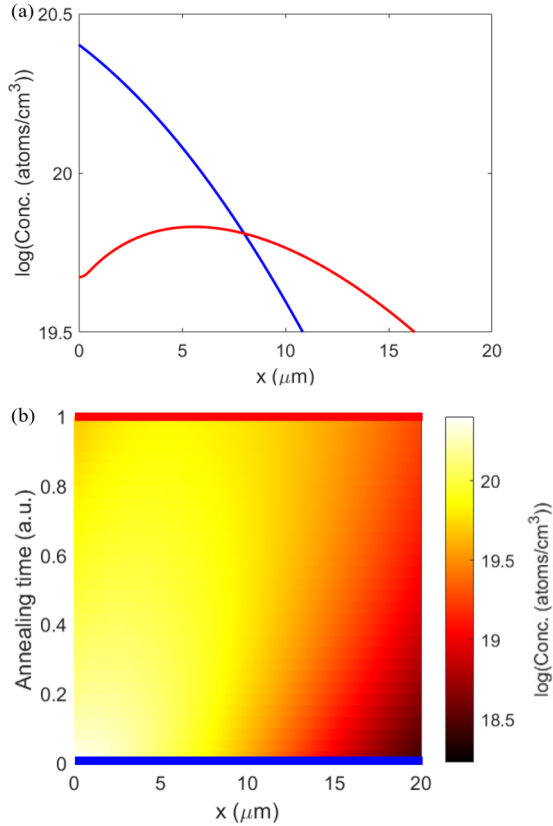

Figure 2: (a) Solution to the Eq. 1 and Eq. 2 before (blue) and after annealing (red). (b) Concentration colormap evolution of the initial condition (blue line) of Eq. 1 advanced in time towards completion of the annealing step (red line).

Despite the ability to capture the form of the diffusion profile, a detailed understanding of the sink term, boundary conditions and diffusion coefficients must be pursued with their temperature dependencies. Such a diffusion model with determined parameters could engage modern theories of RF superconductivity to enhance accelerating fields [6, 9]. Because of the diffusion lengths involved at 800 °C for a few minutes, lengthy depth profiles must be carried out.

OXYGEN ALLOYING

Recently Posen *et al.* [34] showed that heat treatments at ~300 °C for a few hours produced quality factors rivalling those of N alloyed cavities. Ito *et al.* [35] showed that heat treatment of cavities between 300–400 °C resulted in a rise of the quality factor followed by a decay of the quality factor upon higher temperature heat treatments. Such a result is consistent with a hypothesis that an alloying agent had been introduced and diffused away. SIMS measurements [27] of samples heat treated between 140–350 °C showed an influx of oxygen at ~0.1 at. % and consistent with Ciovati's model of native oxide dissolution and oxygen diffusion [36] and the breakdown of the native oxide measured by XPS [37].

The dissolution of oxide can be described by

$$Nb_2O_5 \xrightarrow{k} 2NbO_2 \quad (3)$$
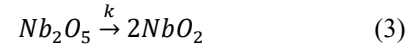
which obeys the rate law

$$-\frac{dA}{dt} = k(T(t))A \quad (4)$$

where reactant A represents Nb₂O₅. To test the model beyond the analysis presented in [27], samples were vacuum heat treated with a ramp rate of 1 °C/min to a maximum temperature and then allowed to cool at 1 °C/min or slower. Sample temperatures measured during vacuum heat treatment are shown in Fig. 3(a). To model an arbitrary temperature profile of a real furnace for the Nb₂O₅ oxide dissolution, we employ the one-dimensional Fick's second law with a time dependent temperature,

$$\frac{\partial c(x,t)}{\partial t} = D(T(t))\frac{\partial c(x,t)}{\partial x^2} + q(t,T(t)). \quad (5)$$

The initial concentration of oxygen in the NbOₓ system is given by the interstitial concentration of oxygen residing in the oxide layer, $c(x,0) = v_0\delta(x)$. Starting from the rate law, Eq. 4, of oxide dissolution, the O produced using a time-dependent temperature is related to the source term by

$$-\frac{dA}{dt} \propto q = u_0 k(T(t)) \exp\left(-\int_0^t k(T(s))\,ds\right)\delta(x) \quad (6)$$

Utilizing the method of reflection and superposition [38], the diffusion equation is subjected to the boundary conditions $c(x = \infty) = c_\infty$ and $c'(x = \infty) = 0$. SIMS depth profiles of those samples are shown in Fig. 3(b). The calculation and fittings in Fig. 3(b) were made with MATLAB using the temperature profiles in Fig. 3(a). The parameters used to generate the plot in Fig. 3(b) are presented in Table 1. The largest spread in parameters comes from the oxygen released from the oxide, u_0, which

MC7: Accelerator Technology

T07: Superconducting RF

is consistent with the spread in the SIMS relative sensitivity factor (RSF) measured elsewhere [29].

Table 1: Parameters used to Generate Fig. 3(b) Fits

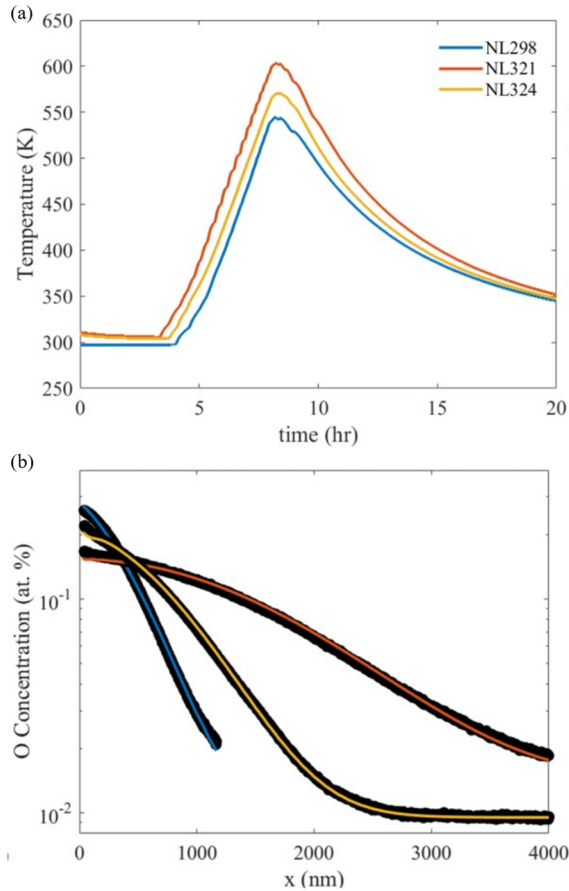|	NL298	NL321	NL324
u_0 (at. % nm)	200	253	167
v_0 (at. % nm)	3.5	3.5	3.5
A $\times 10^9$ (1/s)	1	1	1
E_a (kJ/mol)	132	132	133
D_0 (cm^2/s)	0.076	0.059	0.062
E_{aD} (kJ/mol)	118	120	119

Figure 3: (a) 1 °C/min ramp and ramp down temperature profiles that samples were subjected to. (b) SIMS depth profiles (black circles) of the samples and their theoretical fits (colored lines) as described in the text and using the temperature profiles in (a) within the calculation.

CONCLUSIONS

We have described further modeling of oxygen diffusion from a native oxide dissolution process and nitrogen alloying in Nb. We have tested a model of oxygen diffusion from a native oxide dissolution process found to be consistent with SIMS measurements. This modeling may enable more precise electron mean free path tuning from by selecting a time and temperature. In addition, it may guide a more meaningful experimental parameter space exploration for SRF cavity tests. Compared with the thermal diffusion of N which may suffer from gas conductance [39, 40] and requires challenging multi-micron surface removal, the O-alloying process is conformal due to its oxide covering the surface, allowing Nb cavities of all geometries and Nb thin film resonators [25] to be O-alloyed. These processes could be to create tailored impurity profiles [6, 9] to produce high gradient and high quality factor cavities for future accelerators. Oxygen alloying-based profile tailoring process is patent pending [41].

REFERENCES

[1] D. Gonnella *et al.*, "Industrialization of the nitrogen-doping preparation for SRF cavities for LCLS-II," *Nuclear Instruments and Methods in Physics Research Section A: Accelerators, Spectrometers, Detectors and Associated Equipment,* vol. 883, pp. 143-150, 2018.

[2] D. Gonnella *et al.*, "The LCLS-II HE High Q and Gradient R&D Program", in *Proc. SRF'19*, Dresden, Germany, Jun.-Jul. 2019, pp. 154-158. doi:10.18429/JACoW-SRF2019-MOP045

[3] A. Gurevich *et al.*, "Challenges and opportunities of srf theory for next generation particle accelerators," *arXiv preprint arXiv:2203.08315,* 2022.

[4] A. Gurevich *et al.*, "Surface impedance and optimum surface resistance of a superconductor with an imperfect surface," *Physical Review B,* vol. 96, no. 18, p. 184515, 2017.

[5] T. Kubo *et al.*, "Field-dependent nonlinear surface resistance and its optimization by surface nanostructuring in superconductors," *Physical Review B,* vol. 100, no. 6, p. 064522, 2019.

[6] T. Kubo, "Superheating fields of semi-infinite superconductors and layered superconductors in the diffusive limit: structural optimization based on the microscopic theory," *Superconductor Science and Technology,* vol. 34, no. 4, p. 045006, 2021.

[7] T. Kubo, "Effects of Nonmagnetic Impurities and Subgap States on the Kinetic Inductance, Complex Conductivity, Quality Factor, and Depairing Current Density," *Physical Review Applied,* vol. 17, no. 1, p. 014018, 2022. doi:10.1103/PhysRevApplied.17.014018

[8] T. Kubo, "Multilayer coating for higher accelerating fields in superconducting radio-frequency cavities: a review of theoretical aspects," *Superconductor Science and Technology,* vol. 30, no. 2, p. 023001, 2016.

[9] V. Ngampruetikorn *et al.*, "Effect of inhomogeneous surface disorder on the superheating field of superconducting RF cavities," *Physical Review Research,* vol. 1, no. 1, p. 012015, 2019.

[10] A. Grassellino *et al.*, "Nitrogen and argon doping of niobium for superconducting radio frequency cavities: a pathway to highly efficient accelerating structures," *Superconductor Science and Technology,* vol. 26, no. 10, p. 102001, 2013.

[11] A. Romanenko *et al.*, "Ultra-high quality factors in superconducting niobium cavities in ambient magnetic fields up to 190 mG," *Applied Physics Letters,* vol. 105, no. 23, p. 234103, 2014.

[12] D. Gonnella *et al.*, "Nitrogen-doped 9-cell cavity performance in a test cryomodule for LCLS-II," *Journal of Applied Physics,* vol. 117, no. 2, p. 023908, 2015.

[13] P. Dhakal, "Nitrogen doping and infusion in SRF cavities: A review," *Physics Open,* p. 100034, 2020.

[14] P. Dhakal *et al.*, "Effect of high temperature heat treatments on the quality factor of a large-grain superconducting radio-frequency niobium cavity," *Physical Review Special Topics-Accelerators and Beams,* vol. 16, no. 4, p. 042001, 2013.

[15] G. Ciovati *et al.*, "Decrease of the surface resistance in superconducting niobium resonator cavities by the microwave field," *Applied Physics Letters,* vol. 104, no. 9, p. 092601, 2014.

[16] G. Ciovati *et al.*, "Superconducting radio-frequency cavities made from medium and low-purity niobium ingots," *Superconductor Science and Technology,* vol. 29, no. 6, p. 064002, 2016.

[17] J. Maniscalco *et al.*, "The importance of the electron mean free path for superconducting radio-frequency cavities," *Journal of Applied Physics,* vol. 121, no. 4, p. 043910, 2017.

[18] D. Gonnella *et al.*, "Impact of nitrogen doping of niobium superconducting cavities on the sensitivity of surface resistance to trapped magnetic flux," *Journal of Applied Physics,* vol. 119, no. 7, p. 073904, 2016.

[19] A. Gurevich *et al.*, "Effect of vortex hotspots on the radio-frequency surface resistance of superconductors," *Physical Review B,* vol. 87, no. 5, p. 054502, 2013.

[20] M. Checchin *et al.*, "Frequency dependence of trapped flux sensitivity in SRF cavities," *Applied Physics Letters,* vol. 112, no. 7, p. 072601, 2018.

[21] G. Ciovati *et al.*, "High field Q slope and the baking effect: Review of recent experimental results and new data on Nb heat treatments," *Physical Review Special Topics-Accelerators and Beams,* vol. 13, no. 2, p. 022002, 2010.

[22] D. C. Ford *et al.*, "First-principles calculations of niobium hydride formation in superconducting radio-frequency cavities," *Superconductor Science and Technology,* vol. 26, no. 9, p. 095002, 2013.

[23] F. Barkov *et al.*, "Direct observation of hydrides formation in cavity-grade niobium," *Physical Review Special Topics-Accelerators and Beams,* vol. 15, no. 12, p. 122001, 2012.

[24] D. C. Ford *et al.*, "Suppression of hydride precipitates in niobium superconducting radio-frequency cavities," *Superconductor Science and Technology,* vol. 26, no. 10, p. 105003, 2013.

[25] A.-M. Valente-Feliciano, "Superconducting RF materials other than bulk niobium: a review," *Superconductor Science and Technology,* vol. 29, no. 11, p. 113002, 2016.

[26] S. Posen *et al.*, "Nb3Sn superconducting radiofrequency cavities: fabrication, results, properties, and prospects," *Superconductor Science and Technology,* vol. 30, no. 3, p. 033004, 2017.

[27] E. M. Lechner *et al.*, "RF surface resistance tuning of superconducting niobium via thermal diffusion of native oxide," *Applied Physics Letters,* vol. 119, no. 8, p. 082601, 2021.
doi: 10.1063/5.0059464

[28] J. W. Angle *et al.*, "Advances in secondary ion mass spectrometry for N-doped niobium," *Journal of Vacuum Science & Technology B, Nanotechnology and Microelectronics: Materials, Processing, Measurement, and Phenomena,* vol. 39, no. 2, p. 024004, 2021.

[29] J. W. Angle *et al.*, "Improved quantitation of SIMS depth profile measurements of niobium via sample holder design improvements and characterization of grain orientation effects," *Journal of Vacuum Science & Technology B, Nanotechnology and Microelectronics: Materials, Processing, Measurement, and Phenomena,* vol. 40, no. 2, p. 024003, 2022.

[30] D. Gonnella *et al.*, "Improved N-Doping Protocols for SRF Cavities", in *Proc. IPAC'16*, Busan, Korea, May 2016, pp. 2323-2326.
doi:10.18429/JACoW-IPAC2016-WEPMR025

[31] D. A. Gonnella, "The fundamental science of nitrogen-doping of niobium superconducting cavities," Ph.D. thesis, Phys. Dept., Cornell University, 2016.
https://www.classe.cornell.edu/rsrc/Home/Research/SRF/SrfDissertations/DanielGonnellaThesis_final.pdf

[32] J. T. Clenny *et al.*, "Nitridation kinetics of niobium in the temperature range of 873 to 1273 K," *Metallurgical Transactions A,* vol. 11, no. 9, pp. 1575-1580, 1980.

[33] A. Taylor *et al.*, "The solid solubility of nitrogen in Nb and Nb-rich Nb-Hf, Nb-Mo and Nb-W alloys: Part I: The binary system Nb-N," *Journal of the Less Common Metals,* vol. 13, no. 4, pp. 399-412, 1967.
doi:10.1016/0022-5088(67)90034-3

[34] S. Posen *et al.*, "Ultralow Surface Resistance via Vacuum Heat Treatment of Superconducting Radio-Frequency Cavities," *Physical Review Applied,* vol. 13, no. 1, p. 014024, 2020.

[35] H. Ito *et al.*, "Influence of Furnace Baking on Q-E Behavior of Superconducting Accelerating Cavities," *Progress of Theoretical and Experimental Physics,* 2021.
doi: 10.1093/ptep/ptab056

[36] G. Ciovati, "Improved oxygen diffusion model to explain the effect of low-temperature baking on high field losses in niobium superconducting cavities," *Applied Physics Letters,* vol. 89, no. 2, p. 022507, 2006.

[37] B. King *et al.*, "Kinetic measurements of oxygen dissolution into niobium substrates: In situ X-ray photoelectron spectroscopy studies," *Thin Solid Films,* vol. 192, no. 2, pp. 351-369, 1990.

[38] J. Crank, *The mathematics of diffusion.* Oxford university press, 1979.

[39] J. F. O'Hanlon, *A user's guide to vacuum technology.* John Wiley & Sons, 2005.

[40] C. E. Reece, J. W. Angle, E. M. Lechner, A. D. Palczewski, F. A. Stevie, and M. J. Kelley, "Modeling O and N Alloying in Nb for SRF Applications", presented at the 13th International Particle Accelerator Conf. (IPAC'22), Bangkok, Thailand, Jun. 2022, paper TUPOTK042, this conference.

[41] A. Palczewski, E. Lechner, and C. E. Reece, "Methods of Controllable Interstitial Oxygen Alloying in Niobium", Non-provisional Patent Application No. 17735172, USPTO, May 3, 2022.

MC7: Accelerator Technology

T07: Superconducting RF